PROCEEDINGS OF SPIE

SPIEDigitalLibrary.org/conference-proceedings-of-spie

# Tunable spectral asymmetry at the facets of a chirped tapered quantum-dot superluminescent diode

Bardella, Paolo, Forrest, Adam, Krakowski, Michel, Cataluna, Maria Ana

Paolo Bardella, Adam F. Forrest, Michel Krakowski, Maria Ana Cataluna, "Tunable spectral asymmetry at the facets of a chirped tapered quantum-dot superluminescent diode," Proc. SPIE 11302, Light-Emitting Devices, Materials, and Applications XXIV, 113020Z (25 February 2020); doi: 10.1117/12.2545903

SPIE.

Event: SPIE OPTO, 2020, San Francisco, California, United States

# Tunable spectral asymmetry at the facets of a chirped tapered quantum-dot superluminescent diode

Paolo Bardella[*a], Adam F. Forrest[b], Michel Krakowski[c], Maria Ana Cataluna[b]
[a]Dipartimento di Elettronica e Telecomunicazioni, Politecnico di Torino, I-10129, Turin, Italy
[b]Institute of Photonics and Quantum Sciences, Heriot-Watt University, EH14 4AS, Edinburgh, UK
[c]III-V Lab, 1 Avenue Augustin Fresnel, Campus de Polytechnique, 91767 Palaiseau, France

## ABSTRACT

A wide spectral asymmetry between the wide and narrow facets of a two-section tapered quantum dot (QD) superluminescent diode (SLD) emitting around 1240 nm was observed and investigated. This asymmetry, as characterized by the mismatch in the center wavelengths of the wide and narrow facet spectra, was found to be tunable and had some dependence on the magnitude of the difference in current densities applied to each section of the device. A maximum spectral mismatch of 14 nm was observed when the current density difference between the two SLD sections was 1.5 kAcm$^2$.This spectral asymmetry presents an unexplored degree of freedom which could be exploited via multiplexing from a single device to optimize spectral bandwidth. Furthermore, potentially useful output powers of up to 50 mW were observed from the narrow facet of the SLD, which could again be exploited via single device multiplexing to increase output power, with little to no cost to spectral bandwidth.
The experimental findings were analyzed using a rate-equation based QD model considering the QD ensemble inhomogeneous broadening, the multilayer chirped active material, the spatial distribution of the QD carriers and the spectral and spatial distribution of the photons in the SLDs. The numerical simulations were able to predict the asymmetric output powers extracted from the SLD facets, mainly to due to different equivalent material losses experienced by the forward and backward fields in the weakly gain guided tapered device. Simulations were also able to predict the spectral distribution of the optical fields at the output facets.

**Keywords:** Superluminescent LEDs, Quantum Dot, tunability, spectral asymmetry, tapered waveguide.

## 1. INTRODUCTION

Superluminescent diodes (SLDs) with large spectral bandwidths and high output powers are attractive sources for numerous applications, including high-speed spectroscopy [1] and optical coherence tomography [2], motivating research into enhancing both output parameters. One method that has been exploited to this end is spectral multiplexing, in which the output from two or more independent SLDs are coupled into a single output fiber to produce very broad optical spectra [3]. One of the advantages of the multiplexing technique is that each SLD within the ensemble does not have to be driven close to its lasing limit to achieve a large cumulative spectral bandwidth and output power. However, a drawback of the multiplexing technique is the increased complexity, cost and footprint associated with utilizing multiple SLDs. An alternative approach to upscaling the spectral bandwidth of SLDs is to implement a multi-section design in which two or more electrically isolated contacts can be independently biased to tune the power and spectral bandwidth by varying the relative current density in each section. The advantages of such an approach have been demonstrated in both narrow ridge [3,4] and tapered [5] SLDs, however, most reports have focused solely on the output from a single facet of the devices.

In this paper we present a comparative investigation of the power and spectral bandwidth output from both facets of a multi-section superluminescent diode (SLD), using a device with a chirped quantum-dot (QD) active region and a tapered waveguide structure. A wide spectral asymmetry between the facet outputs was observed and found to be tunable with current density. Numerical simulations were used to better understand the mechanism behind this asymmetry and pointed towards non-uniform filling of the QD states in each section of the non-uniformly pumped SLD as the primary cause. This spectral asymmetry is a yet untapped degree of freedom which could be used to optimize spectral bandwidth via multiplexing from a single device.

Light-Emitting Devices, Materials, and Applications XXIV, edited by Jong Kyu Kim, Michael R. Krames, Martin Strassburg, Proc. of SPIE Vol. 11302, 113020Z
 · doi: 10.1117/12.2545903

## 2. DEVICE DESIGN

The SLD used in this work had a chirped active region that contained a total of 10 layers of InAs QDs, capped by $In_{0.15}Ga_{0.85}As$ layers and separated by 33 nm GaAs barriers. The thickness of the capping layers was varied throughout the active region in order to dictate the emission wavelength of each QD layer. The three QD layers nearest the p-contact of the SLD were grown with a target ground state central emission wavelength at 1211 nm and were followed by 3 layers with a target emission wavelength of 1243 nm. The final 4 layers in the active region, nearest the n-contact, were grown with a target central emission of 1285 nm.

The waveguide of the SLD had a total length of 6 mm and was composed of three distinct geometrical segments [6]. Starting at the rear of the device, there was a 0.5 mm long and 14 μm wide straight segment which led into a tapered segment with a length of 0.5 mm and a taper angle of 1.5˚. Following on from this was a second tapered segment with a taper angle of 0.4˚ that ran along the remaining 5 mm of the device length, giving a front facet width of 110 μm. This waveguide design was derived based on simulations similar to those reported in [7] with the goal of simultaneously improving the gain and beam quality at the tapered facet. To this end, in addition to the distinct geometry, a shallow ridge was etched at the border of the waveguide to introduce a weak index guiding effect to improve optical confinement.

Two electrically isolated contacts were formed by etching an isolation trench 1.875 mm from the rear facet. This meant that the straight, first tapered and part of the second tapered segment of the waveguide (referred to as the rear section) were pumped through the rear contact while the remainder of the SLD (referred to as the front section) was pumped through the front contact. The rear section had a contact area of $3.3\times10^{-3}$ $cm^{-2}$ while the rear section had a contact area of $6\times10^{-4}$ $cm^{-2}$. Therefore, in order to achieve a uniform current density throughout the device, the current in the front section had to be 5.5 times greater than the current in the rear section. The waveguide of the SLD was tilted by and angle of 7˚ relative to its facets, which were also antireflective-coated, in order to minimize optical feedback and prevent the onset of lasing. Throughout this investigation both contacts of the SLD were driven with CW current sources and a fixed operating temperature of 20˚C was maintained.

## 3. RESULTS

### 3.1 Experimental

To begin, the output power emitted from the front and rear facets of the SLD was measured at various combinations of front and rear section driving current densities. These results are plotted in Fig. 1(a) and (b) and show that significant and potentially useful output powers of up to 50 mW were observed from the rear facet at high values of front and rear section current density. At front and rear section current densities of 1.21 $kAcm^{-2}$ and 1.17 $kAcm^{-2}$ respectively, a maximum superluminescent output power of 137.5 mW was measured from the front facet of the device. The output power measured from the rear facet under these driving conditions was 48.5 mW, which means that there was a total combined output power from both facets of 186 mW. Combining the output powers from both facets of the device offers a potential increase over the front facet power of 35% and would come at little to no cost to spectral bandwidth, unlike increases in output power from increases in driving current.

Using linear interpolation between the data points presented in Fig. 1(a) and (b), the output power from both facets of the SLD under uniform current density driving conditions were determined and are plotted in Fig. 1(c). It is worth noting that even under uniform current density conditions, the output power from the device appeared to be dependent on the direction of propagation.

The output spectra emitted from both facets were investigated and an example of the spectra measured at a fixed rear section current density of 0.17 $kAcm^{-2}$ across a range of front section current densities are shown in Fig. 2. Upon comparing the front and rear facet optical spectra under identical driving conditions, a spectral asymmetry can be seen which, in the case of a fixed rear section current of 0.17 $kAcm^{-2}$, tended to increase with increasing front section current density. From Fig. 2 it can be seen that this asymmetry was largely the result of a blue-shifting front facet spectra with increasing current density relative to fairly static rear facet spectra, likely caused by the changing front section current density at a fixed rear section current density.

This spectral asymmetry appeared to have a strong dependence on the bias conditions applied to the two sections of the SLD, variations in which can lead to changes in gain saturation, QD state filling and junction temperature. To further investigate the impact of front and rear section current density on the output spectra, the center wavelength of the spectral

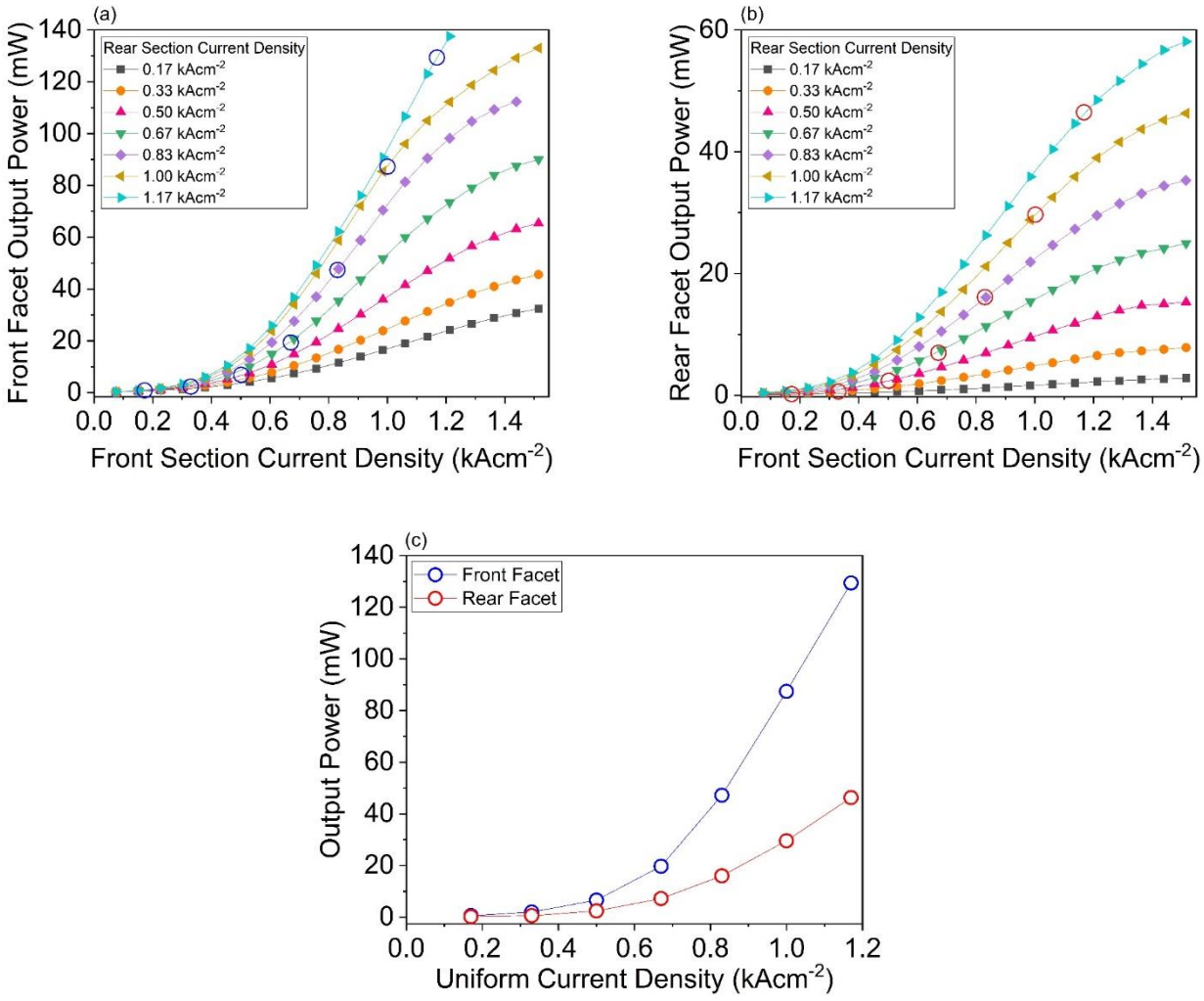


Figure 1. Front (a) and rear (b) facet output power vs front section current density at various fixed rear section current densities. Hollow blue circles in (a) and red circles in (b) mark points of uniform driving current density and correspond to the points plotted in (c) which shows front and rear facet output powers at uniform current densities. Output power values in (c) were calculated from linear interpolation of data in (a) and (b).

feature around 1235 nm, which was present in all spectra observed from both facets, is plotted against front section current density at two fixed rear section current densities in Fig. 3.

At a fixed rear section current density of 0.17 kAcm$^{-2}$, the largest differences in front and rear facet center wavelength were observed and increased with increasing front section current density, ranging from 7 nm to 14 nm across the range of tested front section current densities. At the higher rear section current density of 0.67 kAcm$^{-2}$, shown in Fig. 3(b), the magnitude of the spectral asymmetry between the facets of the SLD was greatly reduced compared to a rear section current density of 0.17 kAcm$^{-2}$. Furthermore, the difference in center wavelength at 0.67 kAcm$^{-2}$ did not simply increase with increasing front section current density as it had done in Fig. 3 (a). The black dashed lines in Fig. 3(a) and (b) indicate the point of uniform current density across the entire device. In both Fig. 3(a) and (b), the largest differences in spectral asymmetry were seen when there was a significant difference in current density applied to the two sections of the device. However, the spectral asymmetry was not solely dependent on the mismatch in the driving condition of the front and rear sections, since, in Fig. 3(b), the spectral asymmetry only appeared to increase when the front section current density was lower than in the rear section and not when it was larger by similar or greater magnitudes. From these results it appeared

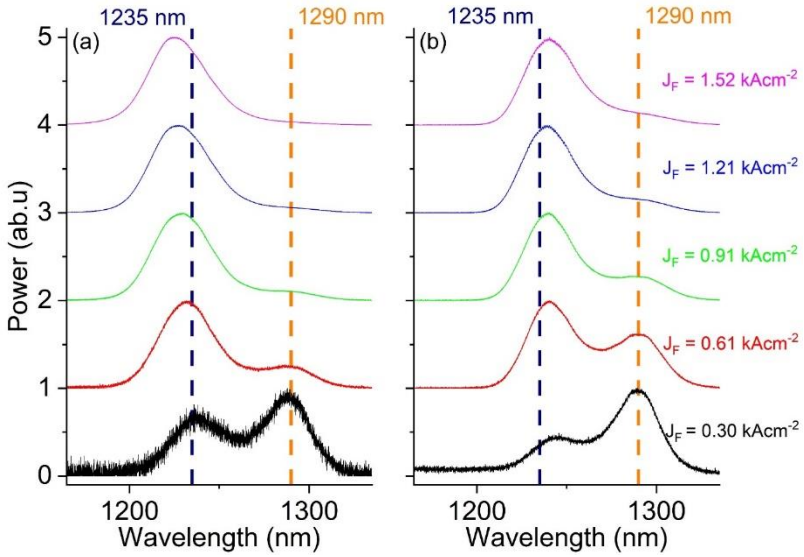


Figure 2. Front (a) and rear (b) facet optical spectra at various front section current densities ($J_F$) and a fixed rear section current density of 0.17 kAcm$^{-2}$.

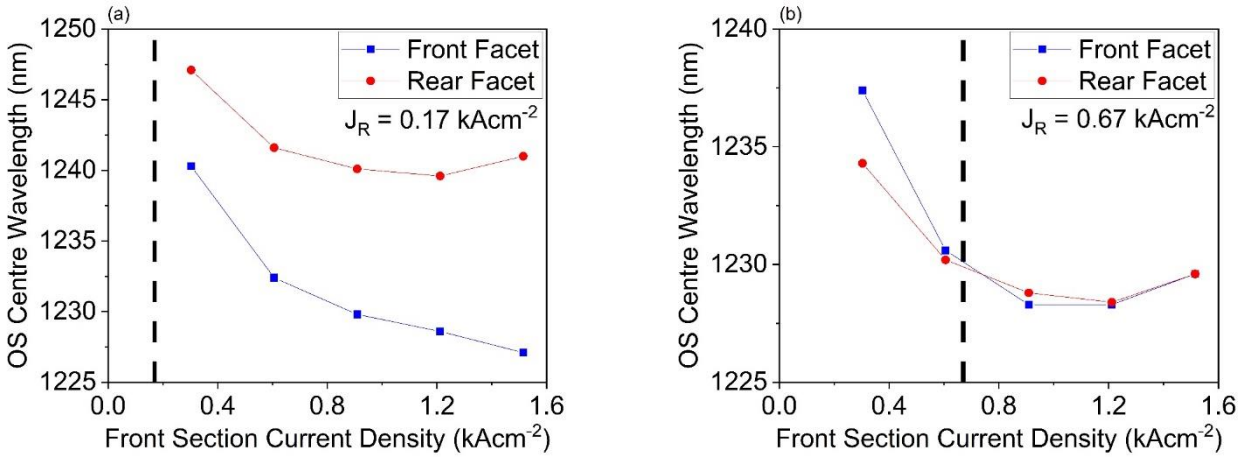


Figure 3. Plots of front and rear facet optical spectra (OS) center wavelength vs front section current density at a fixed rear section current density ($J_R$) of 0.17 kAcm$^{-2}$ (a) and 0.67 kAcm$^{-2}$. Black dashed lines mark the point where the front and rear section current densities were equal.

that the observed spectral asymmetry was dependent on both the mismatch in front and rear section current densities as well as their absolute value.

### 3.2 Numerical Simulation

Numerical simulations, based on an improved version of the model presented in [8], were used in order to understand the origin of the experimentally characterized asymmetry.

In the model, the active QD material is introduced through carrier rate equations describing the longitudinal distribution of the occupation probabilities of the carriers in the ground state (GS), the two excited states (ES1, ES2). Different sets of rate equations are used to describe the various chirped QD layers, characterized by different confined states transition energies; these sets, communicate through a common quasi-2D wetting layer (WL).

The optical spectrum is divided into $N$ uniformly distributed intervals, centered around $E_n$ and with amplitude $2\Delta E$. The spatial evolution of the number of photons $N_{p,n}^{\pm}(z)$ emitted in the energy ranges $(E_n - \Delta E, E_n + \Delta E)$ and propagating in the $\pm z$ directions is described by the differential equation:

$$\pm \frac{\mathrm{d}N_{p,n}^{\pm}(z)}{\mathrm{d}z} = \frac{\beta_{sp}}{2v_g} R_{sp,n}(z) + \left(\Gamma^{\pm}(z) g_n(z) - \alpha_i^{\pm} - \alpha_p(z)\right) N_{p,n}^{\pm}(z) \quad (1)$$

with $R_{sp,n}(z)$ spontaneous emission rate in the selected spectral interval, $v_g$ group velocity, $\beta_{sp}$ spontaneous emission coefficient, $g_n(z)$ material gain, $\alpha_p(z)$ plasma induced losses, proportional to the total WL carriers. The direction-dependent transverse confinement factor $\Gamma^{\pm}(z)$ and material loss $\alpha_i^{\pm}$ can be estimated, e.g., using Beam Propagation Methods simulations taking into account the QD nature of the active material; the forward and backward terms can be different due to the weak field confinement introduced by the gain guided waveguide. The boundary conditions in $z = 0$ and $z = L$ account for the residual reflectivities at the SLD end facets.

In the reported numerical simulation, we assume a 0.65 injection efficiency. the WL transition energy is set to 1.1 eV, while the transition energies for the chirped layers are (1.0239, 0.9976, 0.9650) eV for the GS, (1.0500, 1.0265, 0.9960) eV for the ES1, (1.0690, 1.0508, 1.0333) eV for the ES2; the Full Width at Half maximum of the QD inhomogeneous broadening is 35 meV, resulting in the density of states presented in Fig. 4(a). The maximum material gain is 690 – 750 – 700 cm$^{-1}$ for GS, Es1, and ES2, respectively. The capture times are 5 ps (ES1 to GS), 5 ps (ES2 to ES1), and 12 ps (WL to ES2), while a 10 ns non radiative recombination time is assumed for all the confined states. The propagation losses are $\alpha_i^{+}$ = 1.32 cm$^{-1}$ and $\alpha_i^{-}$ = 3.60 cm$^{-1}$.

The simulated values of the optical power extracted from the rear and the front facets of the device under uniform current injection, calculated with the proposed values of the physical parameters entering the model, are presented in Fig. 4(b), which shows a good agreement with experimental measurements.

Fig. 5(a) shows the evolution with injected current of the net gain in the last ($z$=$L$) slice of the device, when a current density of 0.17 kAcm$^{-2}$ is injected in the rear section. In the same figure, the dashed line indicates the net gain calculated in the first slice ($z$=0). The blue shift observed by the peak of the front section gain is caused by the progressive filling of confined states having higher transition energies in the chirped QD layers, as shown in Fig. 5(b).

When a current of 0.3 kAcm$^{-2}$ is applied in the front section, the optical spectra at the two facets have the same shape and exhibit two peaks around 1250 nm and 1275 nm (Fig. 6a). This result is due to the fact that, at the two considered wavelengths, the net gain in the rear and front sections are similar, as shown in Fig. 6(b).

When a current as high as 1 kAcm$^{-2}$ is injected in the front section, a strong asymmetry is observed in the simulated spectra, in good qualitative agreement with the experiments (Fig. 7a), with peaks around 1210 nm and 1240 nm. The filling of the ES2 in the front section causes a shift in the net gain spectrum, as shown in Fig. 7b. In this condition, at 1240 nm, the rear section is almost transparent, and photons experience an amplification only in the front section. At 1210 nm, the rear section is strongly absorbing, while the net gain in the front section is even larger than the one at 1240 nm. As a result, the optical spectra at the front facet shows a peak at 1210 nm, while the spectrum at the rear facet presents a peak at 1240 nm.

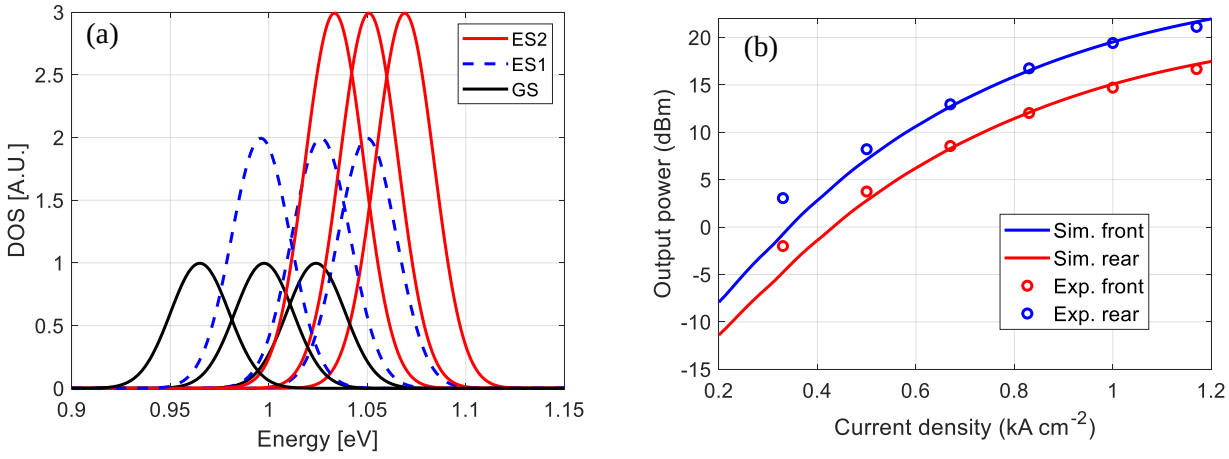


Fig. 4. (a) Normalized density of states of the considered chirped QD material; (b) Simulated (continuous lines) and experimental (markers) powers at the front (blue) and rear (red) facets.

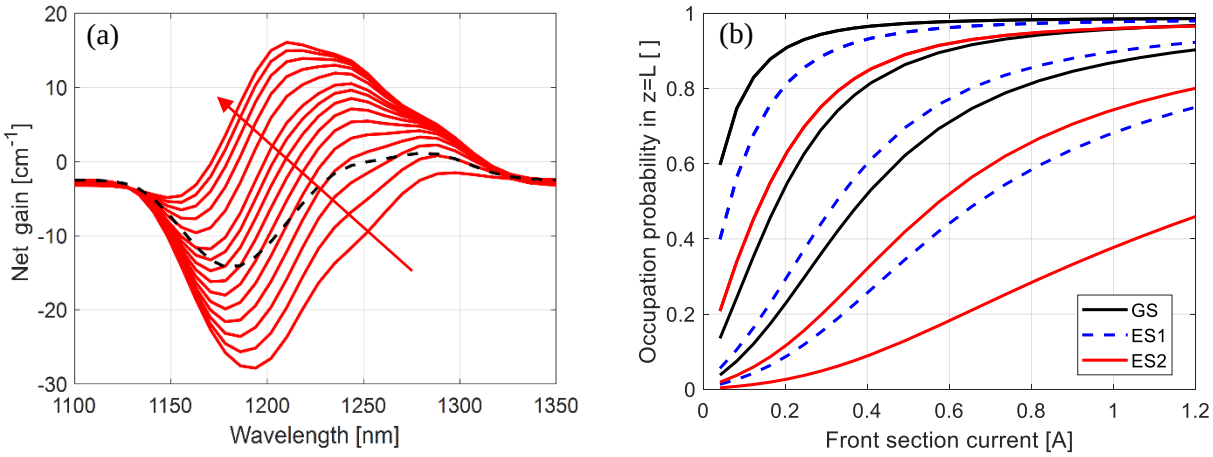


Fig. 5. (a) Average net gain in z=0 (black dashed line) and z=L (red continuous lines). The current in the rear section is 0.17 kAcm$^{-2}$, while the current in the front section is changed from 0.04 kAcm$^{-2}$ to 1.2 kAcm$^{-2}$. (b) Occupation probability in the GS, ES1, and ES2 confined states of the three type of chirped QD layers, for a 0.17 kAcm$^{-2}$ rear section current.

## CONCLUSIONS

We presented a comparative investigation of the spectral asymmetry of the optical spectra measured at the two facets of a two section, QD based, tapered SLD. The spectral asymmetry was highly dependent on the mismatch in the current densities applied to the two electrodes of the device. Numerical simulations, considering the optical properties of the gain guided waveguide and the physics of the active QD medium, were used to justify the asymmetry in terms of different filling of the QD states in the two, non-uniformly pumped, regions. This work shows how both the bandwidth and the optical power of these kind of devices could be improved by multiplexing the power extracted from the two facets. Such spectral asymmetry represents therefore an additional degree of freedom which could lead to a new generation of SLDs with enhanced functionalities.

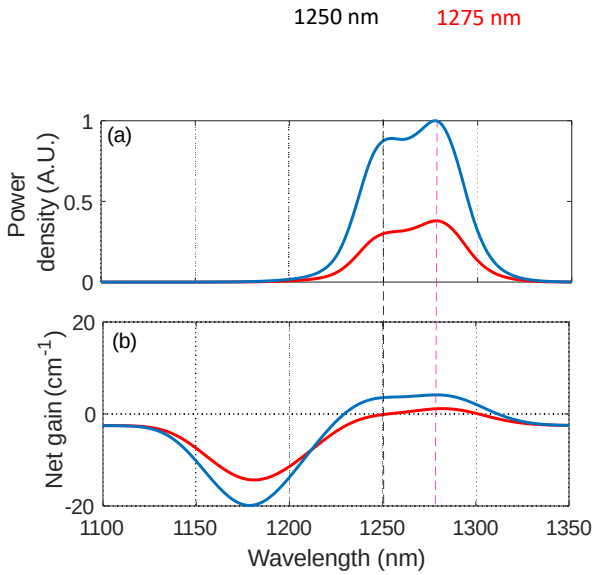


Fig. 6. Simulation results for a rear section current of 0.17 kAcm$^{-2}$ and a front section current of 0.3 kAcm$^{-2}$. (a) Rear (red line) and front (blue line) output power spectra. (b) Net gain in z=0 (red line) and in z=L (blue line).

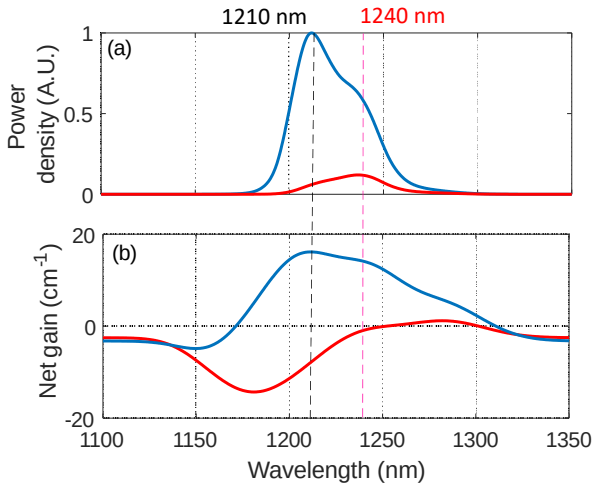


Fig. 7. Simulation results for a rear section current of 0.17 kAcm$^{-2}$ and a front section current of 1 kAcm$^{-2}$. (a) Rear (red line) and front (blue line) output power spectra. (b) Net gain in z=0 (red line) and in z=L (blue line).

## REFERENCES


[1] W. Denzer et al., "Near-infrared broad-band cavity enhanced absorption spectroscopy using a superluminescent light emitting diode," Analyst 134(11), 2220-2223 (2009).

[2] T. H. Ko et al., "Ultrahigh resolution optical coherence tomography imaging with a broadband superluminescent diode light source," Optics Express 12(10), 2112-2119 (2004).

[3] Y. C. Xin et al., "1.3-μm Quantum-Dot Multisection Superluminescent Diodes with Extremely Broad Bandwidth," IEEE Photonic Technology Letters 19(7), 501-503 (2007).

[4] P. D. L. Greenwood et al., "Tuning Superluminescent Diode Characteristics for Optical Coherence Tomography Systems by Utilizing a Multicontact Device Incorporating Wavelength-Modulated Quantum Dots," IEEE Journal Selected Topics in Quantum Electronics 15(3), 757-763 (2009).

[5] X. Li et al., "Experimental investigation of wavelength-selective optical feedback for a high-power quantum dot superluminescent device with two-section structure," Optics Express 20(11), 11936-11943 (2012).

[6] A. F. Forrest et al., "High-power quantum-dot superluminescent tapered diode under CW operation," Optics Express 27(8), 10981-10990 (2019).

[7] T. Xu et al., "Beam propagation method simulation and analysis of quantum dot flared semiconductor optical amplifiers in continuous wave high-saturation regime," IET Optoelectronics 6(2), 110-116 (2012).

[8] P. Bardella et al. "Modeling of Broadband Chirped Quantum-Dot Super-Luminescent Diodes," IEEE Journal Selected Topics in Quantum Electronics 15, 785-791 (2009).